An One-dimensional Continuum Model of Direct Closed Head Impact

by

Y. King Liu, Ph.D.

D. U. von Rosenberg, Ph.D.

Biomechanics Laboratory

Tulane University Schools

of Medicine and Engineering

New Orleans, Louisiana 70112

ABSTRACT

This paper is part of our systematic effort to investigate the phenomena of traumatic head injury. It deals with a fluid-filled rigid container, moving with an initial velocity, striking a rigid wall through a spring and dashpot in parallel, so that an impulsive load is applied to the ensemble. This particular abstraction of the direct head impact phenomena appears to be ideal as a bridge between the simplistic one degree-of-freedom and the complex two- or three-dimensional continuum models of the same.

An exact closed-form (wave propagation) small-time solution for the linear problem associated with the above model was obtained and reported elsewhere. Using the exact solution to the posed problem as a basis, a computer-aided finite-difference numerical solution was obtained for the system. The field descriptions of the fluid pressure and container acceleration depended on a small number of dimensionless parameters. These are: (1) The ratio of the velocity of the skull container (just prior to impact) to the wave speed in the cerebrospinal fluid and brain; (2) the brain to skull mass ratio; (3) the damping factor of the skull materials and (4) the brain to skull stiffness ratios. The head injury potential of a given impact is assessed as a function of the system response. Container acceleration is not a good index of the injury potential.

INTRODUCTION

Because of the special vulnerability of the head to traumatic injury, there have been many models proposed which served either to correlate the observed experimental injury data and/or to delineate the injury mechanism. In the former category are usually simplistic lumped-parameter models, which are based on the notion that in any given impact situation, one can usually discern these elements: mass, elasticity, dissipation and nature of the input pulse. The solution of the differential equation associated with either a single- or two-degree-of-freedom problem yields the relationship between the elements of the model. The system parameter inputs are then found through mechanical (usually driving-point) impedance measurements. Assuming a damage criterion, e.g., the spring always breaks at a certain force level, the solutions to the ordinary differential equations then allow for the plotting of the theoretical impact tolerance curves. The correct tolerance curve is that one which "best fits the observed histopathological data." Typical of the more recent application of this idea to closed head trauma is the paper of Stalnaker et al. [1].

The major advantage of the simple oscillator type models is the ease of solution and hence of use -- there being so few parameters in the model. On the other hand, its principal deficit is its inability to account for the where, when and why of the injury mechanism. To overcome this disadvantage, a parallel series of continuum models have been proposed to relate the injury mechanism to the mechanical parameters of the problem. These generally involve the axisymmetric dynamics of fluid-filled rigid or elastic spherical shells. These models have been recently reviewed by Goldsmith [2] and Liu [3] and will not be reiterated in the interest of brevity. These two- or three-dimensional models, because of their continuum nature, involve a much larger number of dimensionless parameters. The complexity of its mathematical solution often tends to obscure the physics of the problem.

Recently, Hayashi [4] proposed a one-dimensional continuum model, which appeared to be quite promising as a bridge between the simplistic lumped-parameter and the complex two- or three-dimensional continuum models because it has a reasonably small number of parameters and still has an identifiable

and plausible injury mechanism. He idealized the closed head impact problem as a fluid-filled, rigid but massless vessel with an attached spring striking a rigid wall. The vessel represents the skull; the fluid, the brain and cerebrospinal fluid (CSF) and the spring, the composite elastic properties of the helmet, skull, hair, skin and the elasticity of the real wall. He obtained an infinite series solution to the problem. For small values of time, his given solution was very slowly convergent, if at all, and hence was unsuitable for numerical work. However, when he restricted the problem to either very soft or very hard impacts, a one-term approximation was adequate to obtain the pressure field and the time-history of the container acceleration. Liu [3] gave a closed-form exact solution for the problem posed by Hayashi [4] in terms of wave propagation. These results showed that the softer the impact the better the Hayashi [4] approximation. Very soft impacts denote situations where the elasticity of the fluid is large compared to that of the lumped spring of the container. As the impact became harder, attempts to reconcile the infinite series solution to the exact one, by increasing the number of terms in the series, failed completely.

The present paper clarifies this lack of self consistency by adding to the Hayashi [4] formulation the container mass and its dissipation. That the container (skull) mass is not negligible can be shown by the following considerations. The average human head weighs about 4.5 kg. Its cranial cavity has a mean volume of 1,500 cm^3 according to Blinkov and Glezer [5]. Assuming an average specific weight of 1.02 $gr./cm^3$ for the brain matter and CSF, we get a fluid weight of about 1.5 kg. Thus the "brain" to "skull" weight ratio is $\mu = 1.53/3.00 \simeq 0.5$. Even if one were to go to the extreme of using dried skull bone weighing about 300 gm only, e.g., in the experiments of Roberts et al. [6] the weight ratio is at best $\mu = 1.5/0.3 = 5$. In the Hayashi [4] model μ was considered to be infinite, i.e., the container is massless. In the animal experiments of Stalnaker et al. [1], the mass ratio was also about 0.5. The justification for the inclusion of damping in any real system is quite obvious. Stalnaker et al. [1] have indicated that the brain is critically damped.

A One-dimensional Continuum Model

A. Formulation

The present model is an improved version of the one-dimensional continuum model for closed head injury due to Hayashi [4]. The system consists of a rigid container (skull) of mass m containing an elastic fluid (brain and CSF). The container is attached to a spring k and damper d in parallel. The spring and damper represent the composite elastic and dissipative properties of the helmet, hair, skin, skull and the real wall. Thus, the closed head trauma problem is idealized as the impact of a fluid-filled, rigid container attached to a spring-dashpot element striking a rigid wall, see Figure 1. The governing differential equation of the fluid is the wave equation:

$$\ddot{u}_{\tilde{t}\tilde{t}} + \ddot{\xi}_{\tilde{t}\tilde{t}} = c^2 \ddot{\xi}_{\tilde{x}\tilde{x}} \qquad (1)$$

where $\ddot{u}$ = the rigid-body displacement of the container

$\tilde{t}$ = the time

$\tilde{\xi}(\tilde{x},\tilde{t})$ = the displacement of the fluid at location $\tilde{x}$ relative to the container

$c = (B/\rho)^{\frac{1}{2}}$ = wave speed in the fluid

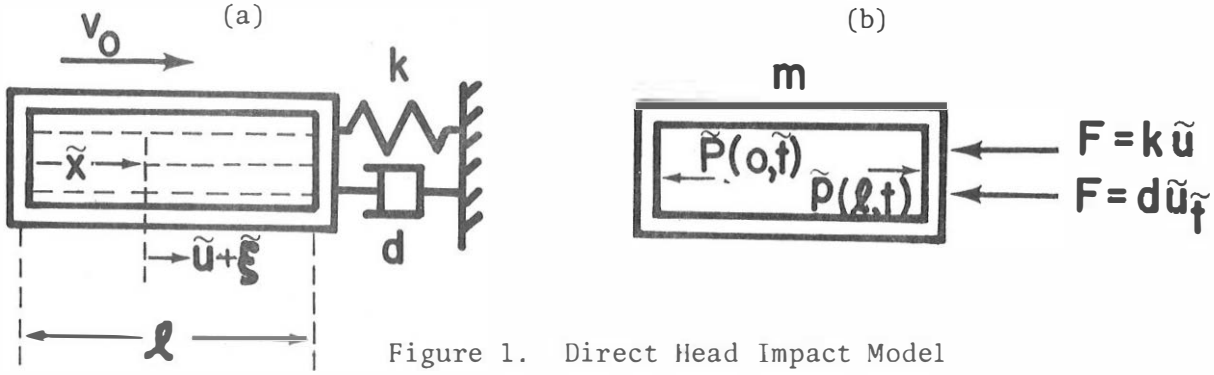

Figure 1. Direct Head Impact Model

B = the bulk modulus of the fluid

ρ = density of the fluid.

The subscript notation is used to denote partial differentiation and the hatted ~ variables designate physical quantities. The initial and boundary conditions are respective by:

$$\tilde{\xi}(\tilde{x},0) = \tilde{u}(0) = 0 \; ; \; \tilde{\xi}_{\tilde{t}}(x,0) = 0 \; ; \; \tilde{u}_{\tilde{t}}(0) = v_o \tag{2}$$

$$\tilde{\xi}(0,\tilde{t}) = \tilde{\xi}(\ell,t) = 0$$

$$m\tilde{u}_{\tilde{t}\tilde{t}} + d\tilde{u}_{\tilde{t}} + k\tilde{u} = AB\left[\tilde{u}_{\tilde{x}}(0,t) - \tilde{u}_{\tilde{x}}(\ell,t)\right], \tag{3}$$

where v_o = velocity of the container just prior to impact

ℓ = the length of the fluid "rod"

m = mass of the container

d = lumped damping coefficient of the container

k = lumped spring constant of the container

A = cross-sectional area of the fluid "rod"

Equations (1), (2) and (3) are valid prior to the rebound of the container, i.e., as long as contact with the wall is maintained. When the spring force becomes zero, loss of contact between the container and wall is impending, hence the rebound condition is

$$k\tilde{u} > 0$$

Equation (3) expresses the dynamic equilibrium of the container and is obtained from a simple free-body diagram analysis, shown in Figure 1b. Using the following nondimensional parameters:

$$u = \tilde{u}/\ell \; ; \; \xi = \tilde{\xi}/\ell \; ; \; t = c\tilde{t}/\ell$$

$$V = v_o/c \; ; \; \omega_n^2 = k/m \; ; \; \zeta = d/2m\omega_n \; ; \; k_f = BA/\ell \tag{5}$$

$$\mu = m_f/m \; ; \; \kappa = k/k_f \; ; \; \Omega^2 = \omega_n \ell/c = \kappa\mu,$$

where V = velocity ratio, ζ = damping ratio, μ = mass ratio and κ = stiffness ratio. The nondimensional differential equation and associated initial and boundary conditions are:

$$u_{tt} = \xi_{tt} = u_{xx} \tag{6}$$

$$\left.\begin{aligned} &\xi(x,0) = u(0) = 0 \ ; \ \xi_t(x,0) = 0 \ ; \ u_t(0) = V \\ &\xi 0,t) = \xi(1,t) = 0 \end{aligned}\right\} \tag{7}$$

and

$$\Omega^2 u + 2\Omega\zeta u_t + u_{tt} = \mu\left[\xi_x(0,t) - \xi_x(1,t)\right] \tag{8}$$

The nondimensional pressure $P(x,t) = - \xi_x(x,t)$.

The coupled system of ordinary and partial differential equations given in (6) - (8) was solved exactly by Liu [7] using the method of Laplace Transformation. The behavior, i.e., the pressure field, container acceleration and displacement, are tracked for every wave traversal. Unfortunately, as the number of wave traversals increased, the exact solution became increasingly unwieldy. To this extent the exact solution is suitable only for the small time region, e.g., three to four wave traversals were given in (7). The exact solution showed that $P(x) = - P(1 - x)$ for all t, i.e., the pressure in the container is skewsymmetric about $x = \frac{1}{2}$, where the pressure is zero. Thus, (8) can be simplified to

$$\Omega^2 u + 2\zeta\Omega u_t + u_{tt} = - 2\mu P(0,t), \tag{9}$$

since $P(0,t) = - P(1,t)$. Also, we need only calculated the solution in the interval $0 \leq x \leq \frac{1}{2}$.

B. An Important Special Case

The form of (9) suggests very strongly that the motion of the container is similar to that of a simple spring-mass-dashpot system. The motion is modified by the fluid pressure in the container. In fact, the complex motions and field fluctuations are best discussed by comparison with the following special case.

Suppose one neglects the fluid-solid interaction, i.e., the head is considered only as a rigid-body of mass $m + m_f$. The solution to such a problem is well-known and we repeat it here only because we need to solve it in the length- and time-scales of the full problem. Denote the rigid body displacement of the combined container and fluid masses by $\tilde{y}(\tilde{t})$, then we get the usual ordinary differential equation and its associated initial conditions:

$$\left.\begin{aligned} &(m + m_f)\, \tilde{y}_{\tilde{t}\tilde{t}} + d\tilde{y}_{\tilde{t}} + k\tilde{y} = 0 \\ &\tilde{y}(0) = 0 \ ; \ \tilde{y}_{\tilde{t}}(0) = v_o \end{aligned}\right\} \tag{10}$$

We nondimensionalize (10) by adding $y = \tilde{y}/\ell$ to those already defined in (5) to yield

$$\left.\begin{aligned} &y_{tt} + 2\alpha\omega y_t + \omega^2 y = 0 \\ &y(0) = 0 \ ; \ y_t(0) = V \end{aligned}\right\}, \tag{11}$$

where the new constant coefficients are related to those in (5) by:

$$\left.\begin{aligned} &\alpha = \zeta/(1 + \mu)^{\frac{1}{2}} \\ &\omega^2 = \Omega^2/(1 + \mu) \end{aligned}\right\} \tag{12}$$

The solution to (11), according to Thomson [8], is:

$$\frac{y(t)}{V} = \frac{e^{-\alpha\omega t}}{\omega(1-\alpha^2)^{\frac{1}{2}}} \sin[\omega(1-\alpha^2)^{\frac{1}{2}}t] \tag{13}$$

$$-\frac{y_{tt}(t)}{V} = \frac{\omega e^{-\alpha\omega t}}{(1-\alpha^2)^{\frac{1}{2}}} \cos[\omega(1-\alpha^2)^{\frac{1}{2}}t + \phi] \tag{14a}$$

where $\phi = \tan^{-1}[(2\alpha^2-1)/2\alpha(1-\alpha^2)^{\frac{1}{2}}]$ (14b)

Even in these simple forms, certain important estimates of the full problem can already be made. For example, the rebound occurs when $\sin[\omega(1-\alpha^2)^{\frac{1}{2}}t]$ in (13) is zero, i.e., loss of contact is pending at

$$t_c = \pi/\omega(1-\alpha^2)^{\frac{1}{2}}, \tag{15}$$

where t_c is the contact duration. The maximum acceleration occurs at

$\cos[\omega(1-\alpha^2)\ t + \phi] = 1$ in (14a)

or

$$t_m = -\phi/\omega(1-\alpha^2)^{\frac{1}{2}}, \tag{16}$$

where t_m is the time to maximum acceleration, Figure 2 is a plot of (14) with $-y_{tt}/\omega V$ on the ordinate, ωt as abscissa, and α as the parameter. Note that for $\alpha > 0.5$, the maximum acceleration occurs at $t = 0$ but $\alpha \leq 0.5$, it is away from zero.

What are the effects of the fluid present in the above problem? Since critical negative pressure, e.g., the cavitation pressure, is the criterion of injury in this model, how is the pressure affected by the system parameter variation? Is the reduction of pressure related to the changes in acceleration of the container? How valid is the prevalent notion that as the container acceleration is reduced by a protective device, the injury potential is correspondingly reduced? These are some of the questions which we hope to answer.

Using the exact solution as the standard of comparison, the following change of variable scheme was used. To begin the numerical solution, define the following new variables:

$$v = u_t \ ; \ s = \xi_x \ ; \ w = \xi_t \tag{17}$$

The governing wave equation (5) becomes

$$v_t + w_t = s_x \tag{18}$$

Since cross differentiation must apply, i.e., $\xi_{xt} = \xi_{tx}$, we get

$$s_t = w_x \tag{19}$$

The initial condition (6) becomes

$$\left.\begin{aligned} &s(x,0) = u(0) = w(x,0) = 0 \\ \text{and} \quad &v = V. \end{aligned}\right\} \tag{20}$$

The boundary condition (7) is rewritten as $w(0,t) = w(1,t) = s(\frac{1}{2},0) = 0$ (21)

Equation (9) is transformed into

$$\Omega^2 u + 2\zeta\Omega v + v_t = 2\mu s(0,t) \tag{22}$$

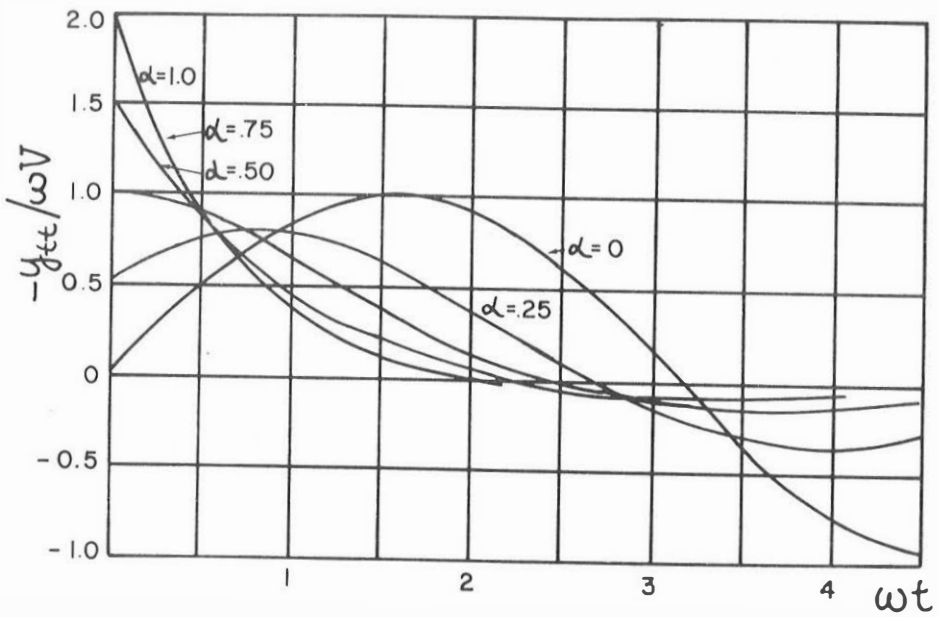

Figure 2. Acceleration-time response for equivalent rigid-body model

C. Finite-Difference Analogs

Set up a finite difference grid as shown in Figure 3. Using centered finite difference analogs, see for example the description in Von Rosenberg [9], we get

$$\left(\frac{\partial s}{\partial t}\right)_{i-\frac{1}{2},n+\frac{1}{2}} \simeq \frac{1}{2}\left[\frac{s_{i,n+1} - s_{i,n}}{\Delta t} + \frac{s_{i-1,n+1} - s_{i-1,n}}{\Delta t}\right] \tag{23}$$

$$\left(\frac{\partial s}{\partial x}\right)_{i-\frac{1}{2},n+\frac{1}{2}} \simeq \frac{1}{2}\left[\frac{s_{i,n+1} - s_{i,n+1}}{\Delta x} + \frac{s_{i,n} - s_{i-1,n}}{\Delta x}\right] \tag{24}$$

Similar analogs exist for w.

Since v is a function of time only, we get

$$\left(\frac{dv}{dt}\right)_{n+\frac{1}{2}} \simeq \frac{v_{n+1} - v_n}{\Delta t} \tag{25}$$

The analogs to (18) and (19) become

$$\left[\frac{v_{n+1} - v_n}{\Delta t}\right] + \frac{1}{2}\left[\frac{w_{i,n+1} - w_{i,n}}{\Delta t} + \frac{w_{i-1,n+1} - w_{i-1,n}}{\Delta t}\right] =$$

$$\frac{1}{2}\left[\frac{s_{i,n+1} - s_{i-1,n+1}}{\Delta x} + \frac{s_{i,n} - s_{i-1,n}}{\Delta x}\right] \tag{26}$$

and

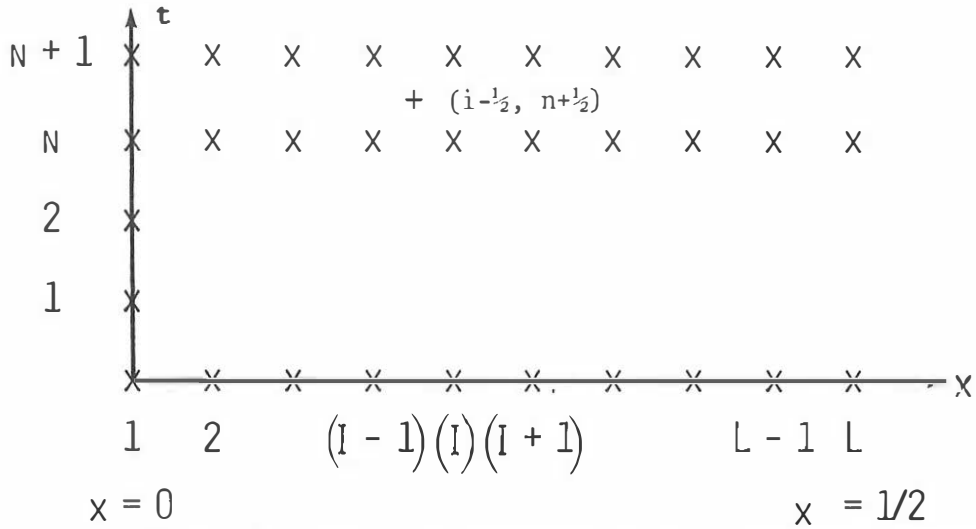

Figure 3. Grid for centered Finite-Difference Method

$$\frac{1}{2}\left[\frac{s_{i,n+1} - s_{i,n}}{\Delta t} + \frac{s_{i-1,n+1} - s_{i-1,n}}{\Delta t}\right] = \frac{1}{2}\left[\frac{w_{i,n+1} - w_{i-1,n+1}}{\Delta x} + \frac{w_{i,n} - w_{i-1,n}}{\Delta x}\right] \tag{27}$$

The initial and boundary conditions (13) and (14) become:

$$s_{i,o} = w_{i,o} \text{ for all i and } u_o = 0 \text{ , } v_o = V \tag{28}$$

$$\left.\begin{aligned} w_{1,n} &= 0 \text{ for all n} \\ w_{L,n} &= 0 \text{ for all n and i = L at x = 1} \\ s_{L,n} &= 0 \text{ for all n and i = L at x = } \tfrac{1}{2} \end{aligned}\right\} \tag{29}$$

Similarly, (22) becomes

$$\Omega^2 u_{n+1} + 2\zeta\Omega v_{n+1} + \left[(v_{n+1} - v_n)/\Delta t\right] = 2\mu s_{i,n+1} \text{ for all n} \tag{30}$$

and

$$v_{n+1} = (u_{n+1} - u_n)/\Delta t, \text{ for all n} \tag{31}$$

To minimize truncation error, we set $\Delta t = \Delta x$ in (26) and (27). Adding these two equations and dividing by 2, one obtains

$$s_{i-1,n+1} + w_{i-1,n+1} = s_{i,n} + w_{i,n} + v_n - v_{n+1}. \tag{32}$$

Subtracting these two equations and dividing by 2, yields

$$- s_{i,n+1} + w_{i,n+1} = - s_{i-1,n} + w_{i-1,n} + v_n - v_{n+1}. \tag{33}$$

Advancing the i index in (32) by unity, we get

$$s_{i,n+1} + w_{i,n+1} = s_{i+1,n} + w_{i+1,n} + v_n - v_{n+1} \tag{34}$$

Adding (33) and (34) and dividing by 2, gives

$$w_{i,n+1} = \left[- s_{i-1,n} + s_{i+1,n} + w_{i-1,n} + w_{i+1,n} \right]/2 + v_n - v_{n+1} \tag{35}$$

Subtract (33) from (34) and divide by 2 gives

$$s_{i,n+1} = (s_{i-1,n} + s_{i+1,n} - w_{i-1,n} + w_{i+1,n})/2 \tag{36}$$

Thus, (35) and (36) specify the values of $s_{i,n+1}$ and $w_{i,n+1}$ from known values at the previous time step. These apply only for $2 \leq i \leq L - 1$. The boundary condition gives $w_{1,n+1} = 0$, then equation (34) yields

$$s_{1,n+1} = s_{2,n} + w_{2,n} - w_{1,n+1} + v_n - v_{n+1} \tag{37}$$

If $i = L$ at $x = 1$, the boundary condition gives $w_{L,n+1} = 0$ and equation (33) can be used to give

$$s_{L,n+1} = s_{L-1,n} - w_{L-1,n} + w_{L,n+1} - v_n + v_{n+1} \tag{38}$$

If $i = L$ at $x = \frac{1}{2}$, the boundary condition gives $s_{L,n+1} = 0$ and equation (33) can be used to obtain

$$w_{L,n+1} = - s_{L-1,n} + w_{L-1,n} + s_{L,n+1} + v_n - v_{n+1} \tag{39}$$

All the values of w and s can be obtained if the value of v_{n+1} is known. This is done through the ordinary differential equation. From

$$v_{n+1} = (u_{n+1} - u_n)/\Delta t,$$

we get

$$u_{n+1} = u_n + (\Delta t)\, v_{n+1} \tag{40}$$

Substituting (37) and (40) into (22) we get

$$\left[\Omega^2(\Delta t) + 2\zeta\Omega + (1/\Delta t) + 2\mu\right] v_{n+1} = \left[(1/\Delta t) + 2\mu\right] v_n +$$

$$\left[- \Omega^2\right] u_n + 2\mu \left[s_{2,n} + w_{2,n} - w_{1,n+1}\right] \tag{41}$$

Equation (41) yields v_{n+1} from all known values.

The problem is thus solved without even the need for the solution of simultaneous equations or iterations.

To summarize the explicit procedure: (a) After the initial and boundary conditions are read into the program, v_{n+1} at the new time step is computed from (41). (b) Compute u_{n+1} from (40). (c) $s_{1,n+1}$ is next calculated from (37) and $w_{L,n+1}$ from (39) or $s_{L,n+1}$ from (38). (d) Finally, the interior values of $s_{i,n+1}$ and $w_{i,n+1}$ are computed in a loop from equations (35) and (36) respectively.

The acceleration can be computed from

$$a_{n+1} = (dv/dt)_{n+1} = (v_{n+1} - v_n)/\Delta t, \tag{42}$$

which is first order correct. From the exact solution we found that the

coefficient of the first truncated term, da/dt, i.e., the changes in the slope of the acceleration of the container, is large near its peaks and valleys making it necessary to have small time steps of $\Delta t = 0.001$ in order to have acceptable accuracy up to the third significant figure. Small time steps increase the time of computation, so a higher-order correct analog was devised to improve the acceleration computation. From the definition of the displacement, velocity and acceleration we obtain the expansion

$$u_{n+1} = u_n + v_{n+1}(\Delta t/1!) - a_{n+1}(\Delta t^2/2!) + (da/dt)_{n+1}(\Delta t^3/3!).... \quad (43)$$

$$v_{n+1} = v_n + a_{n+1}(\Delta t/1!) - (da/dt)_{n+1}(\Delta t^2/2!) + ... \quad (44)$$

$$(da/dt)_{n+1} = (a_{n+1} - a_n)/\Delta t + (d^2a/dt^2)_{n+1}\ \Delta t/2..... \quad (45)$$

Substituting (45) into (44), we get

$$v_{n+1} = v_n + (a_{n+1} + a_n)\ \Delta t/2 - (d^2a/dt^2)_{n+1}(\Delta t^3/12) + ... \quad (46)$$

In turn, we substitute (46) into (43) to get

$$u_{n+1} = u_n + v_n\ (\Delta t) + a_n\ (\Delta t^2/3) + a_{n+1}\ (\Delta t^2/6) - (d^2a/dt^2)_{n+1}\ (\Delta t^4/24) + ... \quad (47)$$

Equation (22) is now written in this new scheme as

$$\Omega^2 u_{n+1} + 2\zeta\Omega v_{n+1} + a_{n+1} = 2\mu\ s_{2,n} + w_{2,n} - w_{1,n+1} + v_n - v_{n+1}$$

Substituting the third-order correct (46) and fourth-order correct (47) into (48) and after some simplification yields

$$\left[\Omega^2(\Delta t^2/6) + (\zeta\Omega + \mu)\ \Delta t + 1\right] a_{n+1} = \left[-\ \Omega^2\right] u_n + \left[-\ \Omega^2\ \Delta t - 2\zeta\Omega\right] v_n + \left[-\ \Omega^2(\Delta t^2/3) - (\zeta\Omega + \mu)\ \Delta t\right] a_n + 2\mu\left[s_{2,n} + w_{2,n} - w_{1,n+1}\right] \quad (49)$$

Equation (49) is our desired result, which is incorporated into the computations in the following way. The steps outlined prior to the improved scheme for acceleration is followed for <u>one time step only</u>, i.e., the terms on the right hand side of (42) are now known values after one time step. Substituting (49) for (41) in the loops completes our numerical procedure. In short, the first-order correct acceleration is used only to <u>start</u> the program, then the higher order correct analogs implicit in (49) are used thereafter. The time step for acceptable accuracy was reduced from 0.001 to 0.01. Taking the usual rule of thumb that the running time is proportional to the square of the before and after step size ratio, we have thus achieved a 100-fold reduction in computational time with the improved acceleration procedure.

Results and Discussion

A. Biomechanical Parameters

As was noted earlier, the input parameters relevant to this model vary considerably depending on the assumptions. We have tried to key our numerical computations to available experimental results:

(a) The mass parameter μ is the ratio of the fluid to container mass. As was discussed previously, it ranged from 0.5 to 5. When a helmet is worn, its value decreases to below 0.5.

(b) The stiffness parameter κ is the ratio of the relative stiffness of the lumped container spring constant and the effective spring constant of the compressible fluid. Following Hayashi [4], if B = 200 kg/mm^2, A = 200 mm^2 and ℓ = 150 mm, we get $k_f = BA/\ell \simeq 267$ kg/mm. The container stiffness used by Hayashi was k = 5 kg/mm, although there is considerable doubt as to its true value. An order of magnitude estimate gives an approximate value of $5/267 \simeq 0.0187$. We have varied this parameter in our study. When a helmet is worn or padding added, we are placing another spring in series with the one for the normal head. The equivalent spring constant is less than the smaller of the two spring constants.

(c) The damping factor ζ is the lumped container damping to its critical damping coefficient. From well-known vibration theory, if $\zeta = 1$, the system is critically damped, $\zeta < 1$, underdamped and $\zeta > 1$, overdamped. Stalnaker et al. [1] conjectured that under vibration and impact the head acts to critically damp the brain. However, their own impedance data indicated it is an underdamped system with $\zeta \cong 0.05$ for the cadaver head to $\zeta = 0.125$ for the Macaca Mulatta. We have done a parametric study on ζ. When another damper is placed in series with the one in place, the equivalent damping is less than the smallest of the two, i.e., the action of dampers in series is the same as a similar combination of springs.

(d) The velocity ratio V compares the speed of the container prior to impact to the wave speed in the fluid. Because of the almost incompressibility of the fluid, its wave speed is a high 150 m/sec.

B. Numerical Results

The results are all presented in dimensionless form. Figure 4 is an isometric view of the pressure time history at different values of x for the mass, stiffness and damping ratios of $\zeta = 0.05$, $\kappa = 0.01$ and $\mu = 0.5$ respectively. We note that the mean pressure variation is almost like a sine wave. The range pressure, i.e., the fluctuations about the mean, are relatively small. The maximum contrecoup negative pressure is P = - 0.029, which occurs at time t = 23.2. Rebound occurs at approximately $t_c \cong 54.5$ when the displacement changes sign. If the mean and range pressures are computed between the peak at t = 23.2 and the next valley at t = 24.10, we get $P_m = (0.0290 + 0.0253)/2 = 0.0271$ and $P_r = (0.0290 - 0.0253)/2 = 0.00185$. Other isometric figures indicate that the maximum pressure occurs at contrecoup and decreases monotonically to zero at x = 0.5; we have, therefore, not continued these isometric views in our parametric studies of the pressure field, but rather have just given the contrecoup result with the understanding that similar qualitative results as given in Figure 4 are obtained.

Figure 5 shows the contrecoup pressure and the container acceleration for $\zeta = 0.1$, $\kappa = 0.01$ and $\mu = 0.5$, i.e., the damping is doubled that shown in Figure 4. The solid line in Figure 5b going through the peaks and valleys indicates that rigid-body acceleration as computed from (14) with the same system parameter values. Note the similarity of this line to the mean pressure values (corresponding to the incompressible case?) in the curve for contrecoup pressure.

Figure 6 shows the contrecoup pressure and its corresponding container acceleration for $\zeta = 0.5$, $\kappa = 0.01$ and $\mu = 0.5$.

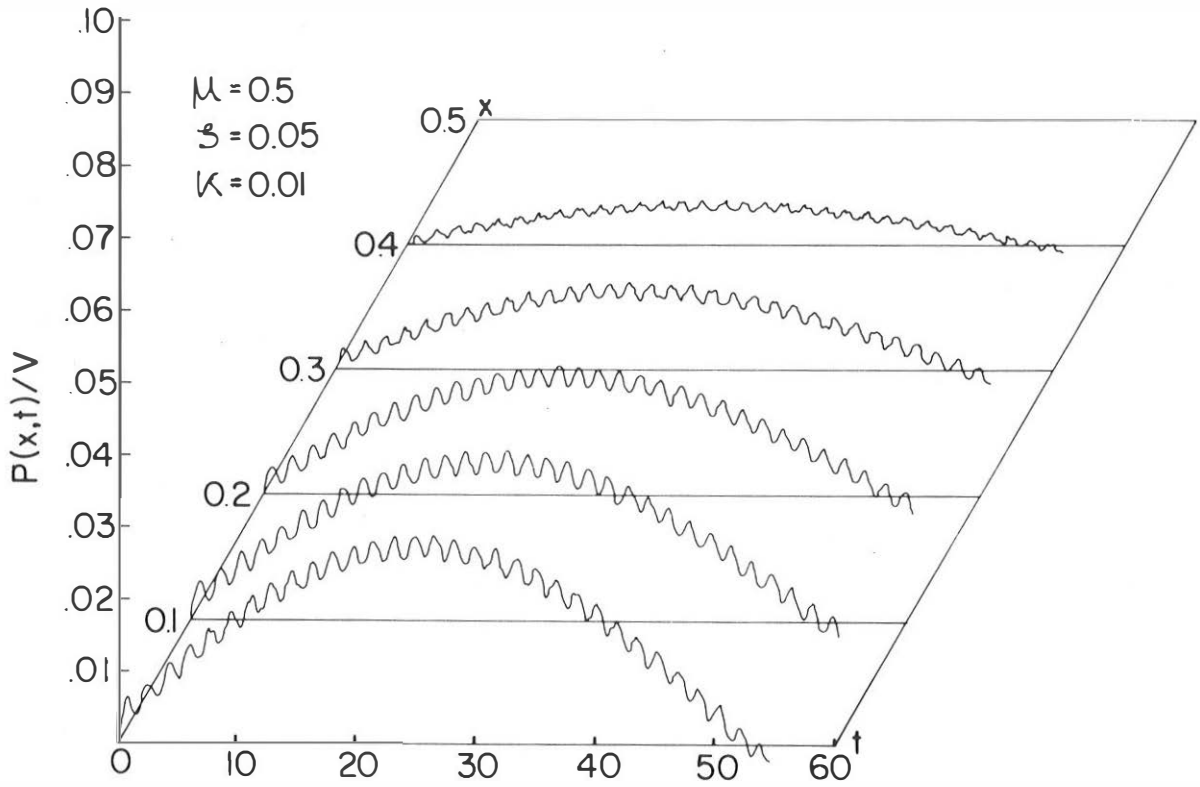

Figure 4. An isometric view of the pressure field as a function of time

The effect of a monotonic damping increases as shown in Figures 4 - 6 indicate clearly that: (a) An increase in the damping ratio increases the range pressure and acceleration, i.e., the peaks and valleys become more prominent. (b) The peak acceleration and contrecoup pressure shift closer and closer to the origin of the time axis as damping is increased. For $[\zeta/(1 + \mu)^{\frac{1}{2}}] > 0.5$, both maximums occur at the origin. For $[\zeta/(1 + \mu)^{\frac{1}{2}}] \leq 0.5$, both maximums are away from the origin. These changes are in complete qualitative accord with the results of the simple spring-mass-dashpot model as shown in Figure 2. (c) The simple oscillator model overestimates the contact duration for $[\zeta/(1 + \mu)^{\frac{1}{2}}] > 0.5$ but for $[\zeta/(1 + \mu)^{\frac{1}{2}}] < 0.5$ the error is relatively small. The reason for this error is attributable to the higher peak velocities attained by the container due to the presence of the fluid, allowing more energy to be dissipated in the damper and thus a quicker spring back.

The other important parameters in our problem besides damping is the mass and stiffness ratio or μ and $\Omega^2 = \kappa\mu$. A 10-fold change on either side of the results given above ($\Omega^2 = 0.005$ and $\mu = 0.5$) will delineate the effects of changes in these parameters. Figure 7 shows the simulation of the experimental impact of fluid-filled human skulls, where $\mu = 5$, $\kappa = 0.001$ and $\zeta = 0.5$ or $\Omega^2 = .005$, e.g., Roberts et al. [6]. Note the high peaks and valleys in both the acceleration and pressure. Even though the amplitude decreases with time, the excursions are still considerable at the time of rebound. Figure 8 compares the effects of the mass ratio change even though $\Omega^2 = \kappa\mu$ is unchanged. The particular cases shown compare (a) $\mu = 0.5$, $\kappa = 0.1$ and $\zeta = 0.5$ with (b) $\mu = 5.0$, $\kappa = 0.01$ and $\zeta = 0.5$. We note that both the absolute and range pressures are much higher in (a) than in (b). Thus, an increase in μ and a decrease in κ and

ζ appear to lower the contrecoup pressure. What happens when one wears a protective helmet? The μ is lowered because m is increased, the κ and ζ are lowered. The ideal helmet or padding for direct head impact is, therefore, one which is as light, as soft and as inviscid as possible.

C. Discussion and Recommendations

The fundamental problem of head protection is to minimize the intracranial pressure response when subjected to a transient excitation. One very obvious improvement in the model is to include the reality of dissipation in the fluid. We expect that many of the peaks and valleys in the pressure and acceleration would damp out when this is done. However, the fluctuations in the small-time region would probably be retained but attenuated.

From the various figures, one can assert that there exists a shape similarity between the acceleration and countercoup pressure curves. This is not surprising since the acceleration of the container can be considered as an input to the wave equation in ξ, see (6). Once the wave enters the fluid it is propagated without dispersion or attenuation until it has traversed the length of the container and is reflected. The interaction with the container occurs only at the boundaries. The contrecoup pressure in turn determines the container dynamics through (9).

We are now in a position to assess the question: In a given impact, if the measured maximum acceleration is lower by changing one of the parameters, what is the effect on contrecoup pressure? The following table, taken from the graphs, is instructive:

Item	μ	κ	ζ	$(A/V)_{max.}$	$[P(0,t)/V]_{max.}$
1)	0.50	0.01	0.5	0.07	0.05
2)	5.00	0.01	0.5	0.17	0.05

Comparison between 1) and 2) show that if μ is decreased 10-fold, the maximum u_{tt} is decreased dramatically and yet the corresponding P(0,t) is unchanged. The common notion that if one can decrease the container acceleration markedly then the probability of injury is correspondingly reduced needs modification. This is in agreement with the result given by Liu [10] that the stress (or pressure or strain) is the criterion of injury and not the acceleration.

A nonlinear optimization problem obviously exists here, i.e., given certain constraints on either the allowable deformation, the weight and the dissipation of the helmet, etc., what force-deflection functions for the spring, i.e., f(u), and force-velocity functions of the damper, i.e., $f(u_t)$, would yield the minimum contrecoup pressure? These considerations are in progress and will be reported in the future.

References

[1] Stalnaker, R.L., Fogle, J.L. and McElhaney, J.H., "Driving Point Impedance Characteristics of the Head," J. of Biomech. 4, pp. 127-139, 1971.

[2] Goldsmith, W., "Biomechanics of Head Injury," Symp. on the Foundations & Objectives of Biomechanics.

[3] Liu, Y.K., "The Biomechanics of Spinal & Head Impact: Problems of Mathematical Simulation," Proc. Symp. Biodyn. Modelling and its Applications, Dayton, Ohio, pp. 701-736, 1970.

[4] Hayashi, T., "Study of Intracranial Pressure Caused by Head Impact," Jour. Fac. of Engr., Univ. of Tokyo, 30, p. 59, 1969.

[5] Blinkov, S.M. and Glezer, I.I., The Human Brain in Figures and Tables, Plenum Press, p. 336, 1968.

[6] Roberts, V.L., Hodgson, V. and Thomas, L.M., "Fluid Pressure Gradient Caused by Impact to the Human Skull," Biomechanics Monograph ASME, p. 223, 1967.

[7] Liu, Y.K., "Package Cushioning for the Human Head," submitted to the Jour. of Appl. Mech. for publication.

[8] Thomson, W.T., Laplace Transformation, 2nd Ed., Prentice-Hall, 1960.

[9] Von Rosenberg, D.U., Methods for the Numerical Solution of Partial Differential Equations, Elsevier, 1969.

[10] Liu, Y.K., "Towards a Stress Criterion of Injury," J. of Biomech. 2, p.145, 1969.

Acknowledgment

This work was supported by the National Institutes of Health through Grant GM 19109-01. The first author is a NIH Research Career Development Awardee (Grant 40723-02).

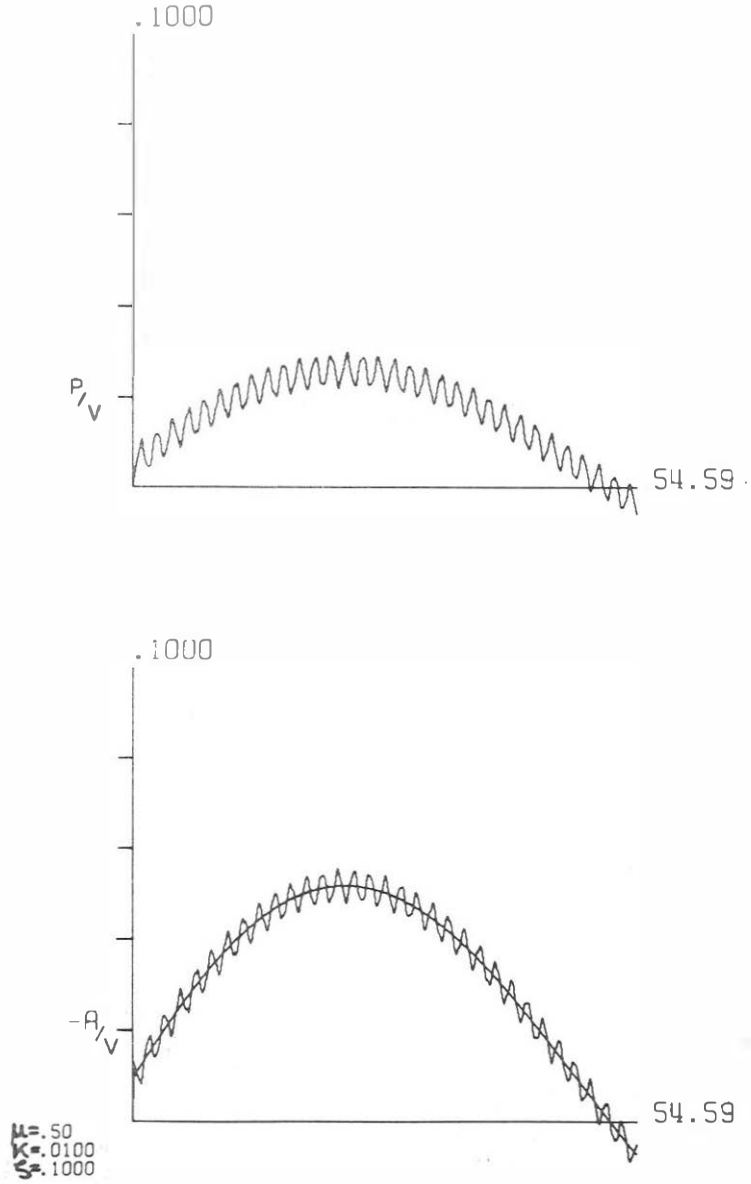

Figure 5. Contrecoup pressure & container-acceleration for μ = .5, κ = .01 & ζ = .1

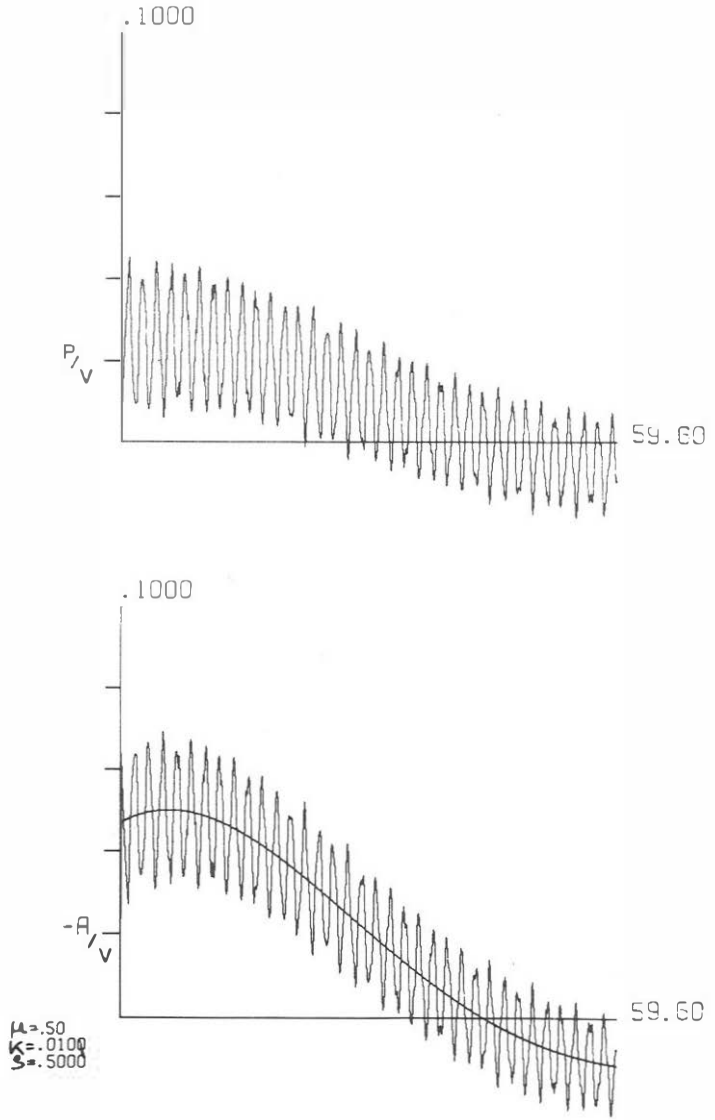

Figure 6. Contrecoup pressure & container-acceleration for μ = .5, κ = .01 & ζ = .5

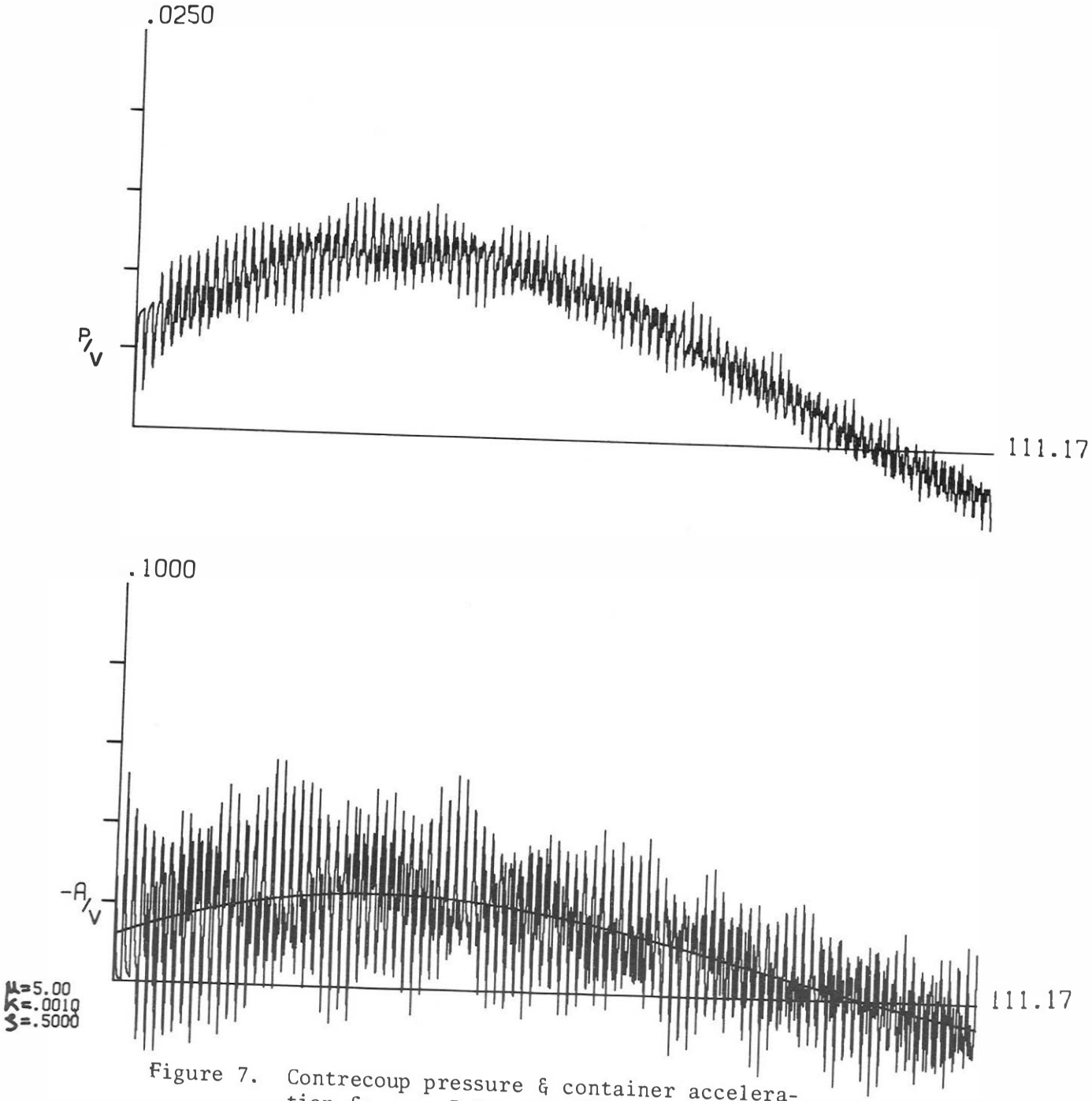

Figure 7. Contrecoup pressure & container acceleration for $\mu = 5.0$, $\kappa = .001$ & $\zeta = .5$

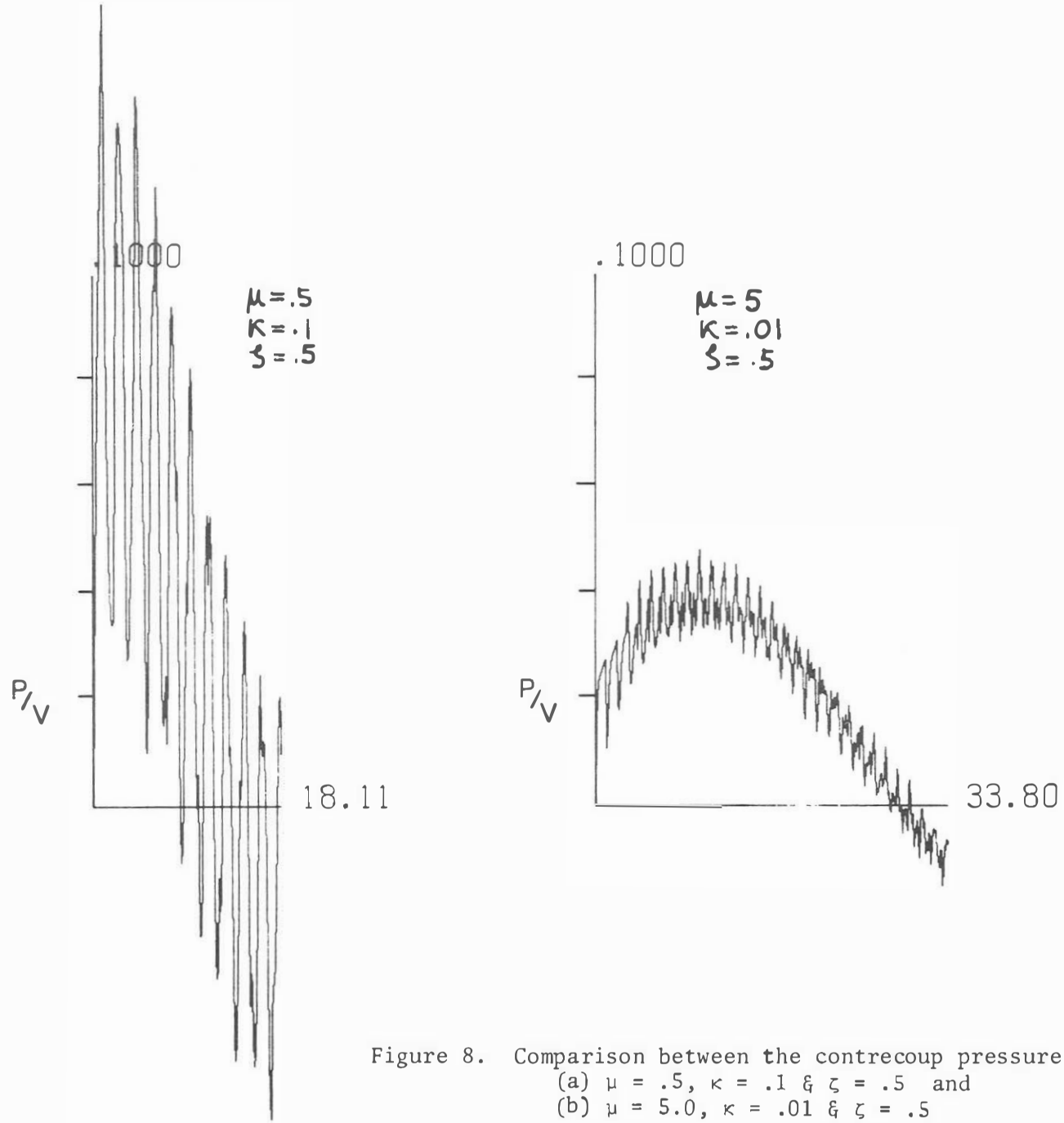

Figure 8. Comparison between the contrecoup pressure for
(a) $\mu = .5$, $\kappa = .1$ & $\zeta = .5$ and
(b) $\mu = 5.0$, $\kappa = .01$ & $\zeta = .5$